Probing the Orientation of β-Lactoglobulin on Gold Surfaces Modified by Alkyl Thiol Self-Assembled Monolayers

ARTICLE *in* THE JOURNAL OF PHYSICAL CHEMISTRY C · MAY 2013

Impact Factor: 4.77 · DOI: 10.1021/jp311964g

6 AUTHORS, INCLUDING:

Jessem Landoulsi
Pierre and Marie Curie University - Paris 6
52 PUBLICATIONS **521** CITATIONS
SEE PROFILE

Souhir Boujday
Pierre and Marie Curie University - Paris 6
55 PUBLICATIONS **747** CITATIONS
SEE PROFILE

Claire-Marie Pradier
Pierre and Marie Curie University - Paris 6
170 PUBLICATIONS **2,830** CITATIONS
SEE PROFILE

Arnaud Delcorte
Université catholique de Louvain
159 PUBLICATIONS **2,025** CITATIONS
SEE PROFILE

THE JOURNAL OF PHYSICAL CHEMISTRY C

Article

pubs.acs.org/JPCC

Probing the Orientation of β-Lactoglobulin on Gold Surfaces Modified by Alkyl Thiol Self-Assembled Monolayers

V. Lebec,[†,‡] J. Landoulsi,[‡] S. Boujday,[‡] C. Poleunis,[†] C.-M. Pradier,[‡] and A. Delcorte*[,†]

[†]Institute of Condensed Matter and Nanosciences (IMCN), Bio and Soft Matter Group (BSMA), Université catholique de Louvain (UCL), Croix du Sud 1, Boite L7.04.01, 1348 Louvain-La-Neuve, Belgium

[‡]Laboratoire de Réactivité de Surface, UMR CNRS 7197, Université Pierre et Marie Curie (UPMC, Paris VI), Site d'Ivry-Le Raphaël, 3 rue Galilée, 94200 Ivry-Sur-Seine, France

Supporting Information

ABSTRACT: The adsorption of a globular protein on chemically well controlled surfaces was investigated in order to correlate its orientation to the surface properties. To this end, three different alkyl thiols, differing by their end group (−COOH, $-CH_3$, and $-NH_2$), were used to build up self-assembled monolayers (SAMs) on gold substrates. β-Lactoglobulin (βLG) was then adsorbed on these SAMs by immersion in a phosphate buffer solution. The surface modification with alkyl thiols and the subsequent adsorption of proteins were characterized *ex situ* by polarization modulated infrared reflection−absorption spectroscopy (PM-IRRAS) and X-ray photoelectron spectroscopy (XPS). The adsorption behavior of proteins was also monitored *in situ* using quartz crystal microbalance with dissipation measurements (QCM-D). Direct evidence regarding the protein orientation in the adsorbed state was obtained by means of time-of-flight secondary ion mass spectrometry (ToF-SIMS). Principal component analysis (PCA), performed on the ToF-SIMS results, enables to separate the samples and shows that the proteins display different distributions of amino acids at the surface depending on the conditioning thiol layer. Our results revealed that the adsorption mode of the protein is influenced by the thiol end groups, and specific orientations of the protein on the surface are proposed for the different substrates.

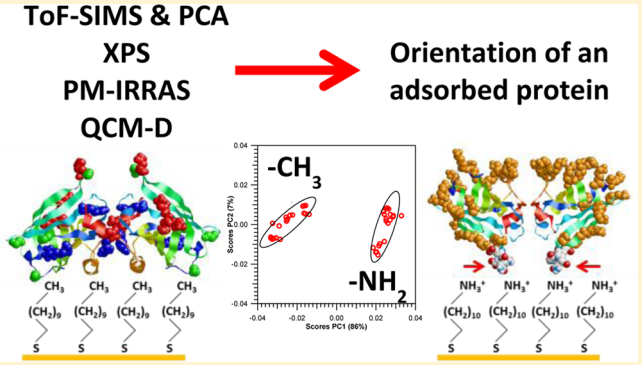

INTRODUCTION

Controlling the reactivity of solid surfaces in biological environments is of crucial importance for new applications in the fields of biosensor and biomaterial researches. In particular, it provides an opportunity to understand and control protein adsorption.[1−3] Generally, the principal consideration is related to the bioactivity of proteins once immobilized, which is mainly governed by their conformation and/or orientation in the adsorbed state. The orientation of proteins on solid surfaces may be greatly influenced by the distribution of charges and hydrophobic areas on the protein and on the surface. For hydrophilic surfaces, adsorption may be mainly driven by electrostatic or hydrogen interactions, while on hydrophobic surfaces, the adsorption process may be dominated by hydrophobic interactions.[4,5] In addition to the orientation, proteins may undergo major deformation upon adsorption, depending on the stability of their 3D structure and physicochemical parameters of the interface; these changes may induce modifications in protein bioactivity.

Self-assembled monolayers (SAMs) of thiolates on gold have been well studied in the past few decades,[6−8] and they constitute adequate substrates for controlled protein adsorption due to the tunability of their chemical properties.[9−13] In previous studies, protein A[14] or β-lactoglobulin[15] were immobilized on thiol SAM-modified gold surfaces, presumably through a covalent link, and characterized by polarization modulated infrared reflection−absorption spectroscopy (PM-IRRAS) and X-ray photoelectron spectroscopy (XPS). Quartz crystal microbalance with dissipation monitoring (QCM-D) has also been widely used to obtain information about the adsorption kinetics of biological molecules[16−18] or antigen−antibody interactions.[19] The main advantage of this technique is to enable *in situ* (i.e., in the liquid phase) a quantitative evaluation of the amount of proteins adsorbed on the surface. Atomic force microscopy (AFM) is also a relevant method to probe the behavior of proteins at solid/liquid interfaces. For instance, AFM has shown great potentialities to image soluble and membrane proteins adsorbed on solid surfaces and provided relevant details at the submolecular level.[20,21]

Moreover, time-of-flight secondary ion mass spectrometry (ToF-SIMS), in the static regime, has become an important tool to probe protein adsorption and orientation because of its

Received: December 5, 2012
Revised: April 12, 2013
Published: May 10, 2013

   dx.doi.org/10.1021/jp311964g | J. Phys. Chem. C 2013, 117, 11569−11577

low sampling depth (a few nanometers).[22] During the SIMS process, proteins are ejected as fragments corresponding to each amino acid.[23−25] Seminal studies of adsorbed proteins in ToF-SIMS were carried out by Lhoest et al., with fibronectin adsorbed on polystyrene, before and after oxygen plasma treatment, and led to the detection of different conformations following the evolution of the amino acids fragment peaks.[26] In more recent studies by Baio et al., the orientation of small proteins adsorbed on SAMs was probed by looking at ratios of amino acid fragment peak intensities known to be localized on certain parts of the protein.[27,28]

However, the direct interpretation of ToF-SIMS spectra remains difficult due to the large and complex information they contain. Consequently, principal component analysis (PCA) was introduced to analyze the ToF-SIMS results and identify the amino acid fragments relevant for the separation of several samples and the elucidation of the orientation of an adsorbed protein. This methodology was successfully applied to detect conformational changes of albumin on polycarbonate membranes[25] and to detect the presence of insulin competitively adsorbed with albumin on various polymers.[29,30] Other studies determined the "head-on" or "end-on" orientation of antibodies on substrates only differing by their charge.[31]

In this study, the correlation between the chemical properties of the surface (e.g., hydrophobicity and surface charge) and the adsorption of a protein, β-lactoglobulin (βLG), is explored. Using ToF-SIMS and PCA, our main goal is to determine the orientation of the protein on these different surfaces. Conformational changes in the adsorbed protein will not be investigated or characterized in this work since βLG can reasonably be considered as a "hard" protein,[32] owing to the stability of its tertiary structure. The model substrates chosen for this study were polycrystalline gold surfaces, conditioned with alkanethiol solutions to form SAMs before adsorbing βLG. Using −COOH, $-CH_3$, or $-NH_2$ thiol end groups, molecular layers with different surface chemistries could be prepared. Adsorption was carefully characterized using complementary techniques, in the liquid phase (QCM-D), in air (PM-IRRAS), and in vacuum (XPS and ToF-SIMS), in order to obtain a full picture of βLG adsorption on the three different SAMs. Finally, an orientation is proposed for βLG on the $-NH_2$ and $-CH_3$-terminated SAMs as a result of the PCA calculations performed on the ToF-SIMS data.

MATERIALS AND METHODS

Chemicals. Three inch diameter silicon wafers were metallized with a 5 nm chromium layer (to enhance gold adhesion on the wafer) and 100 nm of gold on top. Before functionalization, wafers were cut into 1 cm^2 samples, cleaned using UV/O_3 treatment for 15 min, and thoroughly rinsed in absolute ethanol before being dried with N_2.

Chemical control of the gold surfaces was obtained by forming self-assembled monolayers (SAMs) of the following alkyl thiols, $HS-(CH_2)_{10}-R$, with R = COOH (11-mercaptoundecanoic acid, 95%, 450561, Sigma-Aldrich), CH_2-NH_2 (11-amino-1-undecanethiol hydrochloride, 99%, 674397, Sigma-Aldrich), or CH_3 (1-undecanethiol, 98%, 510467, Sigma-Aldrich). As previously described in the literature,[6,13] gold samples were immersed in 1 mM thiol solutions in absolute ethanol for 24 h, rinsed twice with ethanol, and dried under N_2 to form SAMs. Samples were then characterized using PM-IRRAS and XPS.

βLG, one of the major whey proteins,[33] is an acidic protein (isoelectric point = 5.1) bearing a high number of acid functions on its surface as shown on its 3D structure.[34,35] It is found in a dimer form in physiological conditions[34] with two monomers of 162 amino acids (a.a.). The total mass of the dimer is about 36 kDa. It has been previously shown that βLG could be immobilized on SAMs-modified surfaces, presumably via a covalent link, after activation of the thiol end groups.[15] In the present work, the different thiol SAMs were immersed in phosphate buffer solution of the protein. βLG was purchased from Sigma-Aldrich (L3908) and has a purity higher than 90%; it was dissolved with no further purification in a phosphate buffer (pH 7.1) at a concentration of 0.1 mg mL^{-1}.

Thiol-functionalized samples were placed in 24-well plates; 1 mL of the protein solution was then added onto the samples for 2 h incubation. Samples were then rinsed with Milli-Q water to remove the excess of salt coming from the buffer, dried in N_2, and analyzed.

PM-IRRAS. Gold samples were placed in the external beam of the FT-IR instrument (Nicolet Nexus 5700 FT-IR spectrometer), and the reflected light was focused on a nitrogen-cooled mercury−cadmium−telluride (MCT) wide band detector. Infrared spectra were recorded at 8 cm^{-1} resolution, with coaddition of 128 scans. A ZnSe grid polarizer and a ZnSe photoelastic modulator are placed prior to the sample to modulate the incident beam between p and s polarizations (HINDS Instruments, PEM90, modulation frequency = 36 kHz). The detector output is sent to a two-channel electronic device that generates the sum and difference interferograms. Those are processed and undergo Fourier transformation to produce the PM-IRRAS signal $(\Delta R/R_0) = (R_p - R_s)/(R_p + R_s)$. Using a modulation of polarization enabled us to perform rapid analyses of the sample after treatment in various solutions without purging the atmosphere or requiring a reference spectrum.

QCM-D. The adsorption of proteins on SAMs was monitored *in situ* by quartz crystal microbalance with dissipation monitoring. Measurements were performed with a Q-Sense E1 System (Gothenborg, Sweden) at a temperature of 22.0 ± 0.1 °C. The crystal used was thin AT-cut gold-coated quartz with a nominal frequency f of 5 MHz (Lot-Oriel, France). Oscillations of the crystal at the resonant frequency (5 MHz) or at one of its overtones (15, 25, 35, 45, 55, and 65 MHz) were obtained when applying AC voltage. The variations of the resonance frequency (Δf) and of the dissipation (ΔD) were monitored during adsorption of proteins. Solutions were injected into the measurement cell using a peristaltic pump (Ismatec IPC-N 4) at a flow rate of 50 μL min^{-1}. Before protein adsorption, a phosphate buffer solution was injected to establish the baseline. The protein solution was then flowed into the measurement cell until the frequency and dissipation signal reached stationary values. Subsequently, rinsing was performed using phosphate buffer solution. The presented data correspond to the third overtone. Mass uptakes Δm were calculated with the Sauerbrey equation[36] assuming the deposited films behave as a rigid layer.

$$\Delta F = -N\frac{\Delta m}{C_f} \tag{1}$$

where C_f (= 17.7 ng cm^{-2} Hz^{-1}) is the mass sensitivity factor at f = 5 MHz and N (= 1, 3, 5, 7, ...) the overtone number.

dx.doi.org/10.1021/jp311964g | J. Phys. Chem. C 2013, 117, 11569−11577

Table 1. Atomic % of C 1s, O 1s, N 1s, S 2p, and Au 4f XPS Peaks As Assigned on (a) Thiols SAMs or (b) after Protein Adsorption

		C 1s					O 1s			N 1s			S 2p			Au 4f
		C-(C,H)	C-(O,N)	COO C=O Amide	(C=O)-OH	C_{tot}	C=O	C-OH	O_{tot}	NH NH_2	NH_3^+	N_{tot}	S-Au	S_{free}	S_{tot}	
-COOH	(eV)	284.8	286.3	287.7	289.1		532.2	533.5					162.3	163.8		
	(a)	37.3	3.1	0.8	3.2	44.5	3.2	2.3	5.5	-	-	0.4	1.2	0.5	1.8	47.7
	+/-	1.3	0.4	0.2	0.5	1.3	0.4	0.4	0.8			0.4	0.1	0.1	0.1	0.8
	(eV)	284.8	286.3	287.8	289.0		532.0	533.5		400.3	402.0		162.4	163.9		
	(b)	38.8	5.1	1.6	3.5	48.9	4.3	2.1	6.4	1.8	0.3	2.1	1.2	0.5	1.7	40.9
	+/-	0.3	0.3	0.1	0.4	0.3	0.3	0.4	0.7	0.1	0.1	0.2	0.1	0.1	0.1	0.1
$-CH_3$	(eV)	284.8	286.3										162.6	163.8		
	(a)	38.8	1.0	-	-	39.8	-	-	0.1	-	-	0.1	1.7	0.5	2.2	57.9
	+/-	2.8	0.2			2.6			0.2			0.1	0.1	0.1	0.1	2.5
	(eV)	284.8	286.3	288.3			531.8	533.2		400.2	402.0		162.4	163.9		
	(b)	38.4	9.5	6.0	-	54.0	5.3	1.2	6.6	5.1	0.2	5.3	1.0	0.4	1.4	32.7
	+/-	0.5	0.2	0.1		0.3	0.2	0.3	0.2	0.2	0.0	0.2	0.1	0.1	0.1	0.2
$-NH_2$	(eV)	284.8	286.3	288.1			531.2	532.8		399.3	401.3		162.0	163.7		
	(a)	45.7	5.3	1.6	-	52.5	5.2	1.3	6.5	1.3	1.8	3.2	1.2	0.9	2.0	35.8
	+/-	2.7	0.5	1.1		1.9	1.9	0.3	1.6	0.6	0.8	0.2	0.1	0.2	0.2	1.3
	(eV)	284.8	286.3	288.1			531.3	532.9		399.9	401.6		162.0	163.8		
	(b)	40.2	9.3	5.2	-	54.7	8.4	1.3	11.2	5.3	0.9	6.2	0.9	0.6	1.5	26.4
	+/-	3.2	0.8	0.6		4.1	0.2	0.1	1.8	0.8	0.2	1.0	0.1	0.2	0.2	3.6

XPS. XPS analyses were performed on a Kratos Axis Ultra spectrometer (Kratos Analytical, Manchester, UK) equipped with a monochromatized aluminum X-ray source (powered at 10 mA and 15 kV) and an eight-channeltron detector. The pressure in the analysis chamber was about 10^{-6} Pa. Photoelectrons were collected along the normal to the sample surfaces. Analyses were performed in the hybrid lens mode. The pass energy of the hemispherical analyzer was set at 160 eV for the survey scan and 40 eV for narrow scans. In the latter conditions, the full width at half-maximum (fwhm) of the Ag $3d_{5/2}$ peak of a standard silver sample was about 0.9 eV. Charge stabilization was achieved by using an electron source (semicircular filament) mounted coaxially to the electrostatic lens column and a charge balance plate used to reflect electrons back toward the sample. The magnetic field of the immersion lens placed below the sample acts as a guide path for the low-energy electrons returning to the sample. The electron source was operated at 1.8 A filament current and a bias of −1.1 eV. The charge balance plate was set at −2.8 V. The following sequence of spectra was recorded: survey spectrum, C 1s, Au 4f, O 1s, N 1s, S 2p, and C 1s again to check for charge stability as a function of time and the absence of degradation of the sample during the analyses. The C-(C,H) component of the C 1s peak of carbon has been fixed to 284.8 eV to set the binding energy scale. The data treatment was performed with the CasaXPS software (Casa Software Ltd., UK). The peaks were decomposed using a linear baseline, and a component shape was defined by the product of a Gauss and Lorentz function, in the 70:30 ratio, respectively. Atomic % were calculated using peak areas normalized on the basis of acquisition parameters after a linear background subtraction, experimental sensitivity factors based on those of Wagner,[37] and transmission factors provided by the manufacturer. Elemental atomic percentages, excluding hydrogen, are provided.

Three rounds of experiments were performed. The first time, one sample per thiol SAMs and two samples after protein adsorption on each SAMs were analyzed. The two next times, one sample per SAMs and one sample after protein adsorption on each thiols SAM were analyzed. XPS analyses were thus performed on three different samples for each SAM and four different samples after protein adsorption. Results presented in Table 1 correspond to the mean of all samples with standard deviation.

ToF-SIMS and PCA. ToF-SIMS measurements were performed with an IONTOF V spectrometer (IONTOF GmbH, Münster, Germany). The samples were bombarded with pulsed Bi^+ or Bi_3^+ ions (30 keV, 45°). Secondary ions were accelerated at 2 kV before entering the analyzer and postaccelerated at 10 kV before detection. The analyzed area was a square of 500 × 500 μm^2, and the data acquisition time was 60 s. With these parameters, the primary ion dose density was lower than 2×10^{11} ions cm^{-2}, well within the static SIMS limit. The mass resolution $m/\Delta m$ at m/z 70 was about 8000 for each measured sample. To study proteins with ToF-SIMS, positive mass spectra were analyzed and calibrated using CH_3^+, $C_2H_3^+$, $C_3H_5^+$, and $C_7H_7^+$ (m/z = 15, 27, 41, and 91).

PCA is used to determine from which peaks the variability between samples is arising after the adsorption of proteins.[38,39] Prior to PCA analysis, a data pretreatment is needed to select the information coming from the proteins on the surface. For this work, 44 peaks corresponding to amino acids fragments in the positive mass spectrum, and giving a signature of adsorbed proteins, were selected. They are displayed in the Supporting Information.[23−25] The mass spectra were first normalized to the sum of selected peaks, to account for fluctuations in secondary ion yield between different spectra, and then mean-centered. PCA calculations were performed using the NESAC/BIO MVA Toolbox (http://mvsa.nb.uw.edu, Dan Graham Ph.D in University of Washington) for MATLAB (The MathWorks, Inc., Natick, MA). Scores are plotted with the 95% confidence limit; the methodology of the script was described by Wagner et al. in 2001.[24]

For all the thiol surfaces, ToF-SIMS measurements have been performed using both Bi^+ and Bi_3^+ projectiles, but only Bi^+ measurements in the positive mode will be presented, provided that they give similar final results as Bi_3^+. In the peak list presented in the Supporting Information, corresponding to amino acid fragments in ToF-SIMS, CH_4N^+ and $C_2H_6N^+$ fragments can be obtained from numerous different amino acids. It is thus not possible to use them to detect differences in the orientation of a protein, and they were excluded from PCA calculations.

dx.doi.org/10.1021/jp311964g | J. Phys. Chem. C 2013, 117, 11569−11577

RESULTS

First the characterization of the formed SAMs, by PM-IRRAS and XPS, is presented. In the second part of the results, the full analysis of the adsorbed protein layers is described using data provided by *in situ* (QCM-D) as well as *ex situ* (PM-IRRAS and XPS) characterizations. Finally, the ToF-SIMS/PCA studies are presented, and preferential protein orientations on the different substrates are proposed.

SAMs Formation and Characterization. The formation of SAMs of −COOH-, $-CH_3$-, and $-NH_2$-terminated alkyl thiols has been characterized using PM-IRRAS (black lines in Figure 1). Bands at 2921 and 2852 cm^{-1} are attributed to the asymmetric and symmetric stretches of CH_2 in the alkyl chain ($\nu^{as}_{CH_2}$ and $\nu^{s}_{CH_2}$), respectively. The positions of these absorption bands suggest the formation of SAMs.[40,41] The small band at 1454 cm^{-1} can be attributed to the scissoring mode of CH_2 in the alkyl chains. The −COOH-terminated SAM is characterized by bands at 1723 and 1407 cm^{-1}, attributed to the stretching vibration of C═O in COOH and to the symmetric stretching of COO^- ($\nu^{C=O}_{COOH}$ or $\nu^{s}_{COO^-}$), respectively. The strong band at 1723 cm^{-1} and weaker one at 1407 cm^{-1} are strong indications that most acidic groups are in the protonated form, coexisting with a few carboxylates. As for the $-CH_3$-terminated surface, bands are observed at 2965 and 2878 cm^{-1}. They correspond to the asymmetric and symmetric stretches in CH_3 ($\nu^{as}_{CH_3}$ and $\nu^{s}_{CH_3}$), respectively. Finally, $-NH_2$-terminated surfaces show large bands at 1638 and 1565 cm^{-1}, attributed to the deformation of the NH or NH_3^+ end groups (δ^{def}_{NH} and $\delta^{def}_{NH_3^+}$) The comparatively stronger band at 1565 cm^{-1} indicates that the amines are predominantly protonated.

In the XPS survey spectra (not shown), peaks corresponding to C, O, N, S, and Au are observed. The atomic % derived from the C 1s, O 1s, N 1s, S 2p, and Au 4f peak areas are presented in Table 1. In Figure 2, the high-resolution XPS spectra in the S 2p, C 1s, and N 1s regions of each thiol sample are presented, before (a) and after (b) adsorption of βLG. The C 1s peak was decomposed into four components: at 284.8, 286.3 (both fixed in energy upon decomposition), 288.0 ± 0.3, and 289.2 ± 0.3 eV. The former one is attributed to carbon only bound to carbon or hydrogen C−(C, H) and the second one to carbon singly bonded to oxygen or nitrogen C−(O, N); the two high binding energy ones are attributed to carbon doubly bonded to oxygen in amides or in carboxylates (C═O amide, COO^-) and to carbon in carboxyl groups (C═O)−OH,[42] respectively. The O 1s peak was decomposed in two components. The first one at lower binding energy was attributed to oxygen doubly bonded to carbon, C═O, in amides or carboxyls and to oxygen in carboxylates,[42] while the second component, at higher binding energy, is likely due to oxygen singly bonded with carbon (C−OH).[42] The positions of these two components vary slightly between samples (see Table 1) but are close to the tabulated values for biomolecules, 531.8 eV for oxygen in an amide or 533.4 eV in a carboxylic acid,[42] especially for the $-CH_3$-terminated samples after βLG adsorption. For the −COOH and $-NH_2$ samples, shifts in the position of the O 1s peaks can be attributed to the chemical environment of the oxygen atoms. The N 1s peak also shows two components: one at 400.0 ± 0.5 eV attributed to amide or amine NH/NH_2 and another at higher energy (401.7 ± 0.5 eV), indicating the presence of protonated amines NH_3^+. The S 2p peak was decomposed in two doublets attributed to sulfur in S−Au bonds, at low binding energy (S $2p_{3/2}$ at 161.8 ± 0.2 eV), thus confirming the chemisorption of thiols to gold, and sulfur not bound to gold, "S_{free}" (S $2p_{3/2}$ at 163.3 ± 0.1 eV). Indeed, all layers include a fraction of thiols not bound to gold, likely interacting via H or hydrophobic interactions with other chemisorbed thiols; the maximum amount of "weakly" bound thiols is observed on the $-NH_2$-terminated layer.

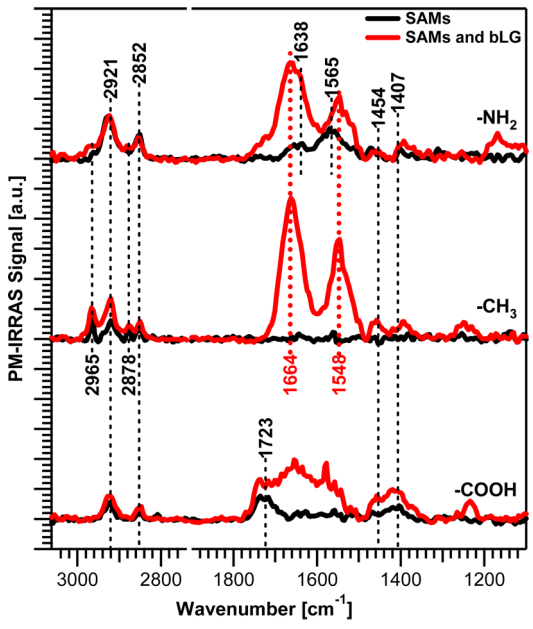

Figure 1. PM-IRRAS measurements before and after βLG adsorption on −COOH-, $-CH_3$-, and $-NH_2$-terminated SAMs.

On the −COOH-terminated surface, COO^- of carboxylates and (C═O)−OH components appear in the C 1s spectrum, with a large excess of the latter (3.2% vs 0.8%), indicating that carboxylic acid functions are predominantly in the protonated form (see Table 1). On the $-CH_3$-terminated surface, the C-(C,H) component is, as expected, predominant, corresponding to the $-CH_2$ in the alkyl chain and the $-CH_3$ termination of the thiol. On the $-NH_2$-terminated SAMs, the presence of a carbon contribution at 288.0 eV corresponding to carbon atoms in carboxylates, the detection of an O 1s signal, and the larger S_{Free} component on the S 2p peak show that this SAM is less organized compared to the $-CH_3$ and −COOH ones. Nevertheless, for the $-NH_2$-terminated surface the N 1s peak displays a small component at low energy, 400.0 ± 0.5 eV (NH/NH_2), and a dominating one at higher binding energy, 401.7 ± 0.5 eV, showing the coexistence of neutral and protonated amines, as already observed on the PM-IRRAS spectrum where the protonated form was also predominant.

In Table 1, the percentages of gold in the different SAMs are 47.7% for the −COOH SAMs, 57.9% for the $-CH_3$, and 35.8% for the $-NH_2$ ones. Those values are in reasonable agreement with what was found in the literature. For thiols with the same chain lengths as the ones used in the present study, Apte et al.[43] report values of 51.5% of gold for the CH_3 and 44.4% for the COOH-terminated SAMs. In another paper, Baio et al.[28] report values of 36.9% of gold for the $-NH_2$ SAMs and 43.7% for the −COOH ones.

Despite the rinsing procedure, the −COOH and $-NH_2$ surfaces still present unbound thiols after formation of the SAMs. However, in our conditions, the overall surfaces show mostly the presence of protonated amine groups for the $-NH_2$-

dx.doi.org/10.1021/jp311964g | J. Phys. Chem. C 2013, 117, 11569−11577

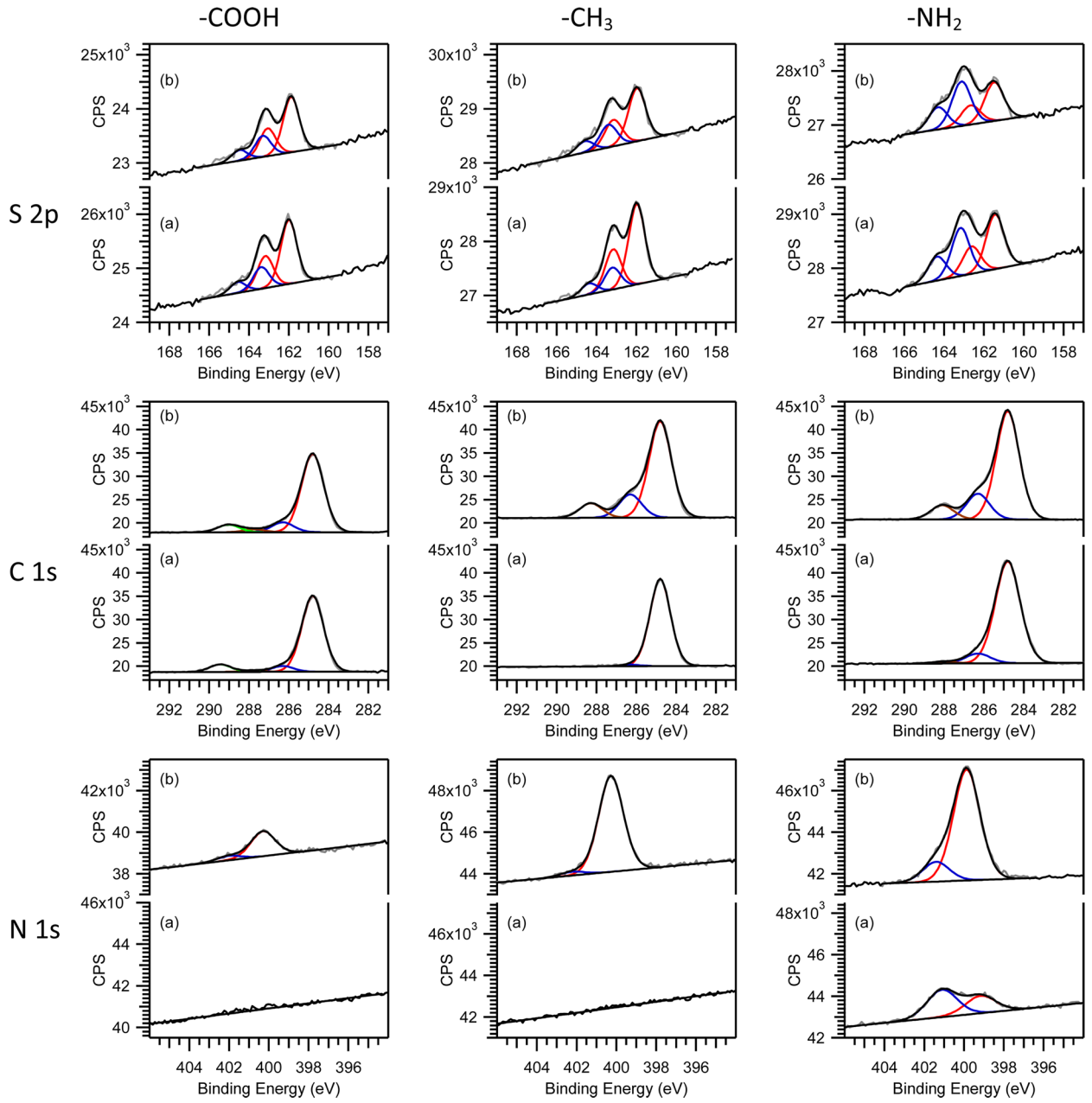

Figure 2. XPS spectrum for the S 2p, C 1s, and N 1s peaks on each different thiol before (a) and after (b) βLG adsorption.

terminated SAM and of a mixture of unprotonated and protonated carboxylic acid groups for the COOH-terminated surface. Finally, a likely hydrophobic surface is obtained using the $-CH_3$-terminated thiols, and two hydrophilic surfaces are obtained with one being negatively charged ($-$COOH SAMs) and one positively charged ($-NH_2$ SAMs). Using these modified surfaces, adsorption of proteins will now be investigated.

***In Situ* Monitoring of Protein Adsorption Using QCM-D.** QCM-D results recorded upon the adsorption of βLG are presented in Figure 3. For each thiol surface, a rapid adsorption of the protein after stabilization is observed with no noticeable variation in the dissipation measurements, suggesting that protein adsorption lead to the formation of a rigid-like structure layer. On the $-$COOH-terminated surface, the adsorbed protein layer is not stable upon rinsing in a phosphate buffer solution (red curve in Figure 3), as shown by the increase in frequency shift, indicating the removal of the proteins. Even for longer rinsing times (not shown here), Δf did not stabilize, indicating a progressive desorption of the proteins. For $-NH_2$, the frequency shift was constant after 20 min of rinsing, indicating no further desorption, while no effect of rinsing was noticeable on $-CH_3$ SAMs.

***Ex Situ* Characterization after Protein Adsorption Using PM-IRRAS and XPS.** Using PM-IRRAS, protein adsorption can be monitored by the presence of the amide I and II bands at ~1664 and ~1548 cm^{-1}. Figure 1 shows that both bands are present on the $-CH_3$- and $-NH_2$-terminated surfaces. Moreover, the higher intensity of these bands on the $-CH_3$ surfaces indicates a greater quantity of proteins adsorbed on the $-CH_3$ than on the $-NH_2$ functionalized samples. On the $-$COOH-terminated surface, no clear amide bands are detected. The small increase of the peak around 1650 cm^{-1} could indicate a low amount of proteins adsorbed on the

dx.doi.org/10.1021/jp311964g | J. Phys. Chem. C 2013, 117, 11569−11577

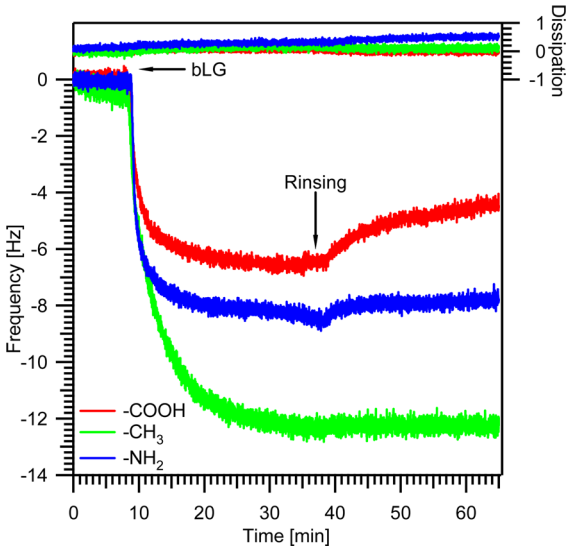

Figure 3. Frequency and dissipation change obtained in QCM-D by adsorption of βLG on $-$COOH-, $-CH_3$-, and $-NH_2$-terminated SAMs.

surface. This can be correlated to the QCM-D results showing that βLG adsorption is reversible upon rinsing on $-$COOH-terminated samples.

XPS confirms the adsorption of the protein on the $-CH_3$ and $-NH_2$ samples (Figure 2b and Table 1). The XPS fingerprint of protein adsorption is the N 1s peak (Figure 4), whose increase is higher on the $-CH_3$- than on the $-NH_2$-terminated surfaces after adsorption, indicating that methyl groups favor the adsorption of proteins. After βLG adsorption on the $-CH_3$ and the $-NH_2$ surfaces, C 1s peak show two contributions growing, at 286.3 and 288 eV, and corresponding to carbon in C$-$(O, N) and C$=$O. These features are characteristic of peptidic bonds. Confirming the QCM-D and PM-IRRAS measurements, the XPS spectra of the COOH-terminated surface shows only a small increase of the C 1s, N 1s, and O 1s peak intensities, suggesting a very low amount of adsorbed proteins.

Exploring the Adsorbed Protein Orientation Using ToF-SIMS and PCA. The first part of this study showed that βLG is adsorbed on the $-CH_3$- and $-NH_2$-terminated SAMs in larger quantities than on the $-$COOH-terminated surfaces. In order to obtain additional information regarding the orientation of the protein after adsorption, indirect techniques such as biorecognition measurements or fluorescent tagging could have been used. Instead, a direct approach was chosen using ToF-SIMS measurements. In principle, ToF-SIMS allows us to retrieve chemical information corresponding to the first nanometers of the protein layer and, therefore, to determine which part of the protein is exposed on each surface. To achieve that goal, ToF-SIMS measurements were treated by applying PCA to the secondary ion peaks corresponding to amino acid fragments.

Multivariate analysis was first performed using samples from the three thiol surfaces, but the mass spectra from the $-$COOH surfaces after βLG adsorption were not clearly separated from the others on the score plot. Indeed, they presented a large dispersion in principal component score plot, probably because of the low amount of adsorbed protein. Thus, PCA calculations were used only for the $-CH_3$ and $-NH_2$ SAMs.

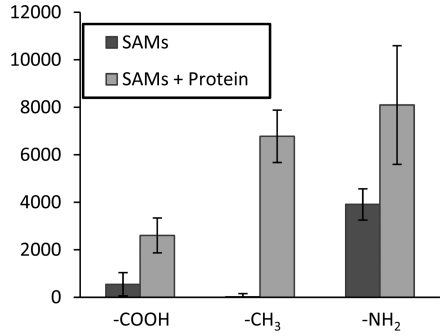

Figure 4. Raw area of N 1s XPS peaks before and after βLG adsorption on $-$COOH-, $-CH_3$-, or $-NH_2$-terminated thiols SAMs.

PCA results on $-CH_3$- and $-NH_2$-terminated surfaces are presented in Figure 5. Samples corresponding to these two surfaces are clearly separated along principal component 1 (PC1), which takes into account 86% of the information contained in the original peak series. Surfaces terminated by $-CH_3$ display negative PC1 scores and $-NH_2$, positive ones. The PC1 loadings are presented in Figure 5b. Large positive or negative loadings point out the amino acid fragments which allow the separation between samples. Fragment ions corresponding to lysine, methionine, proline, and cysteine give the largest positive loadings, while arginine, asparagine, glycine, or glutamic acids give the largest negative ones. Unraveling the link between scores and loadings will determine which amino acids are dominating on ToF-SIMS spectrum of one or the other surface.

Figure 6 presents the average intensity of the considered amino acid fragments after normalization to the sum of all of them, for the $-CH_3$- and $-NH_2$-terminated samples. For peaks presenting large positive loadings in PC1 (Figure 5b), the mean intensity is higher on the $-NH_2$-terminated samples. On the contrary, negative loadings peaks display a higher intensity for the $-CH_3$-terminated surfaces. Thus, along PC1, negative scores correspond to negative loadings (arginine, asparagine, glycine, or glutamic acid) and positive scores to positive loadings (lysine, methionine, proline, or cysteine). To determine the most likely orientation of the protein on each surface, the 3D structure of the protein as well as its adsorption data on each type of surface will be considered.

DISCUSSION

Amount of Adsorbed Proteins. QCM-D data may provide a rough evaluation of the amount of adsorbed proteins. Low dissipation in QCM-D measurements indicates the formation of a "rigid" protein layer on the surface. Accordingly, based on the Sauerbrey model, the mass of adsorbed protein may be estimated (see eq 1). Values of 220 and 140 ng cm^{-2} were obtained when proteins are adsorbed on $-CH_3$ and $-NH_2$ SAMs, respectively. Considering the area of a dimeric βLG[35] as equal to 16 nm^2 in an upright orientation and 32 nm^2 in a flat lying one, the mass per unit area could thus be calculated for a theoretical monolayer coverage, i.e., 380 ng cm^{-2} in an upright orientation and 190 ng cm^{-2} in a flat lying one. From QCM-D, performed in the liquid phase, the calculated mass uptake includes adsorbed proteins and water molecules that bind or hydrodynamically couple to the macromolecules; it is thus overestimated in comparison with other techniques.[44−46] Moreover, the calculated values for monolayer coverage are an extreme case where all the adsorbed

dx.doi.org/10.1021/jp311964g | J. Phys. Chem. C 2013, 117, 11569−11577

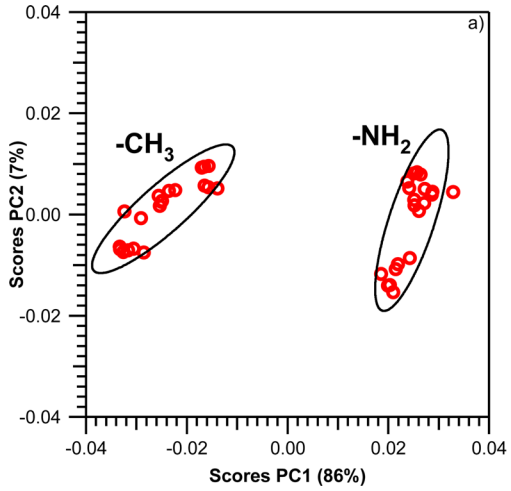

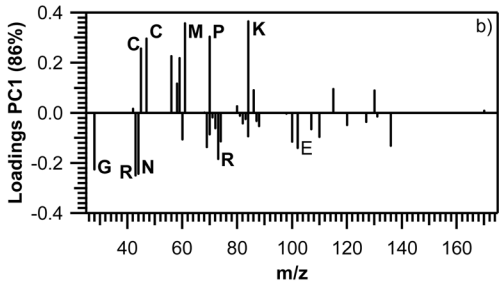

Most important positive and negative loadings

Loadings (+)	Mass	a.a.	Loadings (-)	Mass	a.a.
0.365	84.09	K	-0.249	43.03	R
0.357	61.01	M	-0.243	44.01	N
0.304	70.07	P	-0.226	28.02	G
0.296	47.00	C	-0.185	73.06	R
0.257	44.98	C	-0.140	102.06	E

Figure 5. PCA calculation results on $-CH_3$- and $-NH_2$-terminated SAMS after adsorption of βLG: (a) scores for PC1 and PC2, (b) loadings for PC1 with most important values in the table.

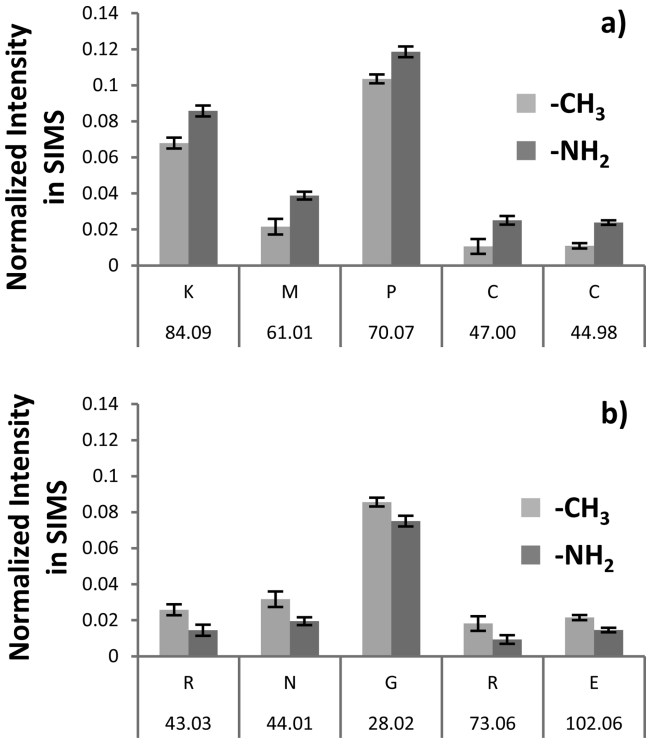

Figure 6. Mean peak intensities for most important positive (a) and negative (b) loadings of PC1.

proteins would be in the same orientation. Since the calculated mass uptakes from QCM-D are overestimated, dimeric βLG should form less than a monolayer on both surfaces.

The amount of adsorbed protein is also probed using XPS, first by comparing the quantity of nitrogen observed in each samples (see Figure 4). In addition, the Au 4f atomic percentage decreases from 57.9% to 32.7% for the $-CH_3$ surfaces and from 35.8% to 26.4% for the $-NH_2$ ones. Ratios between the values of each series are equal to 0.56 and 0.74, respectively. This indicates a stronger attenuation of the signal in the case of the $-CH_3$ SAMs, also revealed by QCM-D and PM-IRRAS, showing that protein adsorption is enhanced on this surface.

Regarding $-COOH$ SAMs, it must be kept in mind that upon adsorption of βLG the pH was maintained by a buffer at 7.1. QCM data suggest weak interactions between the $-COOH$-terminated surface and the protein. This may be attributed to the repulsive interaction between the negatively charged surfaces ($COOH/COO^-$) and the globally negatively charged proteins (isoelectric point = 5.1), while hydrophobic interactions can be neglected. On the $-NH_2$-terminated SAMs, the surface is globally positively charged, thus interacting favorably with the negatively charged proteins, leading to a significant amount of βLG on the surface. The orientation of the βLG molecules on both surfaces will now be discussed in greater detail using ToF-SIMS/PCA results and physicochemical considerations.

Orientation. On the NH_2-terminated SAM, the terminal amine groups were shown to be predominantly protonated (PM-IRRAS and XPS); moreover, from ToF-SIMS and PCA results, lysine corresponds to the main positive loadings, giving positive scores on $-NH_2$-terminated surfaces. Thus, in Figure 7a which shows βLG in the dimer form, with the lysine residues highlighted in gold color, the orientation of the protein is chosen with the lysine residues on top. In contrast, glutamic acid and asparagine have very negative loadings in the PC1. The two red arrows indicate a region rich in these negatively charged or polar a.a. (NH_2-Glu-Asn-Gly-Glu-COOH from residue 62 to 65) in both chains of the dimer. They are logically in the vicinity of the charged surface. Carboxylic acids terminating glutamic acid residues have a pK_a of 4.3. Asparagin is a polar a.a., but its carboxyamide group cannot be ionized. Considering the adsorption pH (7.1), glutamic acid residues should be mainly negatively charged during the process. It is thus proposed that βLG interacts through electrostatic interactions between the Glu-Asn-Gly-Glu sequence and the $-NH_3^+$ end groups on the surface. This is consistent with the expected repulsion between the surface and the lysine-rich regions in βLG.

Unlike the $-NH_2$ surface, the $-CH_3$ surface is purely hydrophobic. In that case, the adsorption mechanism of βLG may involve a monomer−dimer exchange. Wahlgren and Elofsson have reported a mechanism based on the adsorption of dimers favored by lateral interactions with adsorbed monomers.[47] Here two different possible orientations of the protein in the dimer form are proposed based on the PCA

dx.doi.org/10.1021/jp311964g | J. Phys. Chem. C 2013, 117, 11569−11577

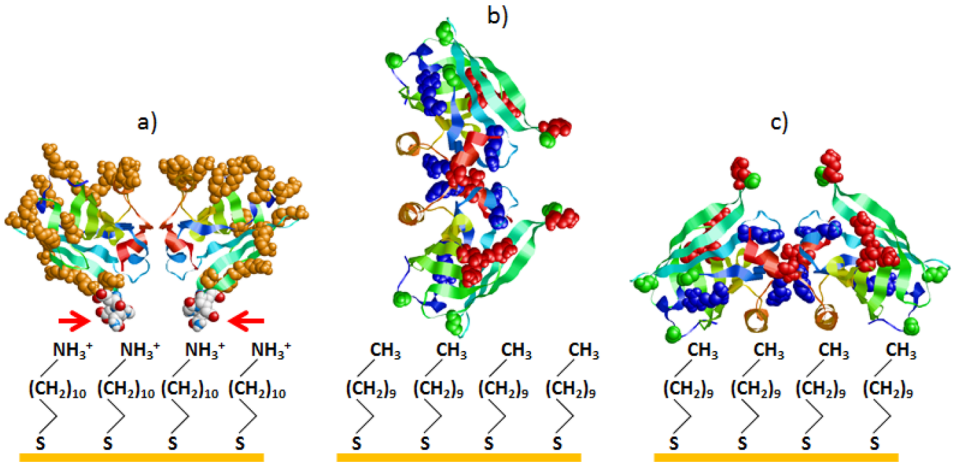

Figure 7. Proposed orientation of βLG on $-NH_2$ (a) and CH_3 (b, c) terminated SAMs. (a) Lysine in gold color and red arrows indicates the ENGE sequence; (b, c) arginine (R) in blue, asparagine (N) in red, and glycine (G) in green.

results. In Figure 7b, the βLG dimer is presented in upright position, exposing a.a. which were relevant for the separation of the $-CH_3$ and $-NH_2$ surfaces in ToF-SIMS measurements (arginine, asparagine, and glycine in blue, red, and green, respectively). This position could be favored by protein−protein interactions with a stabilization of the dimeric form. In Figure 7c the flat lying orientation, in the opposite way as on $-NH_2$ surfaces, is proposed. As previously shown in ToF-SIMS measurements, arginine, asparagine, and glycine are also well exposed at the protein surface in this orientation.

CONCLUSION

Adsorption of βLG was carried out on −COOH-, $-CH_3$-, and $-NH_2$-terminated SAMs of thiolates on polycrystalline gold. Only the $-CH_3$- and $-NH_2$-terminated surfaces showed a clear adsorption of the βLG, with a higher mass uptake on the $-CH_3$-terminated one. The weak interaction of the protein with −COOH surfaces is explained by the fact that both the surface and the protein were negatively charged at the pH used for adsorption.

Regarding the orientation of the protein on both the $-CH_3$ and $-NH_2$ SAMs, a clear separation of the samples was obtained from PCA calculations performed on the ToF-SIMS results. Taking into account the physicochemical condition of adsorption and the molecular structure of the protein, different orientations for the protein have been proposed. According to those results, the βLG would preferentially adsorb in a flat lying position with lysine residues pointing upward on the $-NH_2$-terminated samples due to electrostatic interactions. As for the $-CH_3$-terminated surfaces, two possible orientations are suggested by the ToF-SIMS results, either upright or flat lying, but flipped vertically with respect to the $-NH_2$ surfaces. This interpretation, in agreement with the complementary information obtained from other analytical techniques, is also consistent with the idea that adsorption is driven by hydrophobic interactions.

ASSOCIATED CONTENT

Supporting Information

Table of all amino acids fragments peaks used in PCA calculation. This material is available free of charge via the Internet at http://pubs.acs.org.

AUTHOR INFORMATION

Corresponding Author

*E-mail arnaud.delcorte@uclouvain.be, tel +32 (0) 10 47 35 96 (A.D.).

Notes

The authors declare no competing financial interest.

ACKNOWLEDGMENTS

Victor Lebec acknowledges Université catholique de Louvain for funding through the FSR instrument. This PhD project is held in the framework of the European doctoral school IDS-FunMat. Arnaud Delcorte is a senior research Associate of the Fonds National de la Recherche Scientifique of Belgium. The authors gratefully thank Michel Genet for his help for the XPS measurements and interpretation. The authors also thank Dan Graham, Ph.D., for developing the NESAC/BIO Toolbox used in this study and NIH grant EB-002027 for supporting the toolbox development.

REFERENCES

(1) Kasemo, B. Biological Surface Science. *Surf. Sci.* **2002**, *500*, 656−677.

(2) Castner, D. G.; Ratner, B. D. Biomedical Surface Science: Foundations to Frontiers. *Surf. Sci.* **2002**, *500*, 28−60.

(3) Gray, J. J. The Interaction of Proteins with Solid Surfaces. *Curr. Opin. Struct. Biol.* **2004**, *14*, 110−115.

(4) Norde, W.; Buijs, J.; Lyklema, J. Adsorption of Globular Protein. In *Fundamentals of Interface and Colloïd Science*; Lyklema, J., Ed.; Elsevier Inc.: Amsterdam, 2005; Vol. *V*, p 844.

(5) Rabe, M.; Verdes, D.; Seeger, S. Understanding Protein Adsorption Phenomena at Solid Surfaces. *Adv. Colloid Interface Sci.* **2011**, *162*, 87−106.

(6) Bain, C. D.; Troughton, B. E.; Tao, Y. T.; Evall, J.; Whitesides, G. M.; Nuzzo, R. G. Formation of Monolayer Films by the Spontaneous Assembly of Organic Thiols from Solution onto Gold. *J. Am. Chem. Soc.* **1989**, *111*, 321−335.

(7) Ulman, A. Formation and Structure of Self-Assembled Monolayers. *Chem. Rev.* **1996**, *96*, 1533−1554.

(8) Schreiber, F. Structure and Growth of Self-Assembling Monolayers. *Prog. Surf. Sci.* **2000**, *65*, 151−257.

(9) Prime, K. L.; Whitesides, G. M. Self-Assembled Organic Monolayers: Model Systems for Studying Adsorption of Proteins at Surfaces. *Science* **1991**, *252*, 1164−7.

(10) Ostuni, E.; Chapman, R. G.; Holmlin, R. E.; Takayama, S.; Whitesides, G. M. A Survey of Structure−Property Relationships of

Surfaces that Resist the Adsorption of Protein. *Langmuir* **2001**, *17*, 5605−5620.
(11) Schreiber, F. Self-Assembled Monolayers: from "Simple" Model Systems to Biofunctionalized Interfaces. *J. Phys.: Condens. Matter* **2004**, *16*, R881−R900.
(12) Azioune, A.; Pireaux, J.-J.; Houssiau, L. ToF-SIMS Surface and Interface Characterization of the Immobilized Camel Antibody (cAb) onto SAMs-COOH/Au Substrates. *Appl. Surf. Sci.* **2004**, *231*−*232*, 402−405.
(13) Love, J. C.; Estroff, L. A.; Kriebel, J. K.; Nuzzo, R. G.; Whitesides, G. M. Self-Assembled Monolayers of Thiolates on Metals as a Form of Nanotechnology. *Chem. Rev.* **2005**, *105*, 1103−69.
(14) Briand, E.; Salmain, M.; Compère, C.; Pradier, C.-M. Immobilization of Protein A on SAMs for the Elaboration of Immunosensors. *Colloids Surf., B* **2006**, *53*, 215−24.
(15) Thébault, P.; Boujday, S.; Sénéchal, H.; Pradier, C.-M. Investigation of an Allergen Adsorption on Amine- and Acid-Terminated Thiol Layers. *J. Phys. Chem. B* **2010**, *114*, 10612−10619.
(16) Zhou, C.; Friedt, J.-M.; Angelova, A.; Choi, K.-H.; Laureyn, W.; Frederix, F.; Francis, L. A.; Campitelli, A.; Engelborghs, Y.; Borghs, G. Human Immunoglobulin Adsorption Investigated by Means of Quartz Crystal Microbalance Dissipation, Atomic Force Microscopy, Surface Acoustic Wave, and Surface Plasmon Resonance techniques. *Langmuir* **2004**, *20*, 5870−8.
(17) Weber, N.; Wendel, H. P.; Kohn, J. Formation of Viscoelastic Protein Layers on Polymeric Surfaces Relevant to Platelet Adhesion. *J. Biomed. Mater. Res., Part A* **2005**, *72*, 420−427.
(18) Kim, J. T.; Weber, N.; Shin, G. H.; Huang, Q.; Liu, S. X. The Study of beta-Lactoglobulin Adsorption on Polyethersulfone Thin Film Surface Using QCM-D and AFM. *J. Food Sci.* **2007**, *72*, E214−221.
(19) Zhang, J.; Su, X. D.; O'Shea, S. J. Antibody/Antigen Affinity Behavior in Liquid Environment with Electrical Impedance Analysis of Quartz Crystal Microbalances. *Biophys. Chem.* **2002**, *99*, 31−41.
(20) Alessandrini, A.; Facci, P. AFM: a Versatile Tool in Biophysics. *Meas. Sci. Technol.* **2005**, *16*, R65.
(21) Müller, D. J.; Janovjak, H.; Lehto, T.; Kuerschner, L.; Anderson, K. Observing Structure, Function and Assembly of Single Proteins by AFM. *Prog. Biophys. Mol. Biol.* **2002**, *79*, 1−43.
(22) Delcorte, A.; Leblanc, C.; Poleunis, C.; Hamraoui, K. Computer Simulations of the Sputtering of Metallic, Organic, and Metal − Organic Surfaces with Bi_n^+ and C_{60}^+ Projectiles. *J. Phys. Chem. C* **2013**, *117*, 2740−2752.
(23) Bartiaux, S. Etude de poly(acides aminés) par ToF-SIMS et XPS - Application à l'analyse d'une protéine. Undergraduate Thesis, Université catholique de Louvain, 1995.
(24) Wagner, M. S.; Castner, D. G. Characterization of Adsorbed Protein Films by Time-of-Flight Secondary Ion Mass Spectrometry with Principal Component Analysis. *Langmuir* **2001**, *17*, 4649−4660.
(25) Henry, M.; Dupont-Gillain, C. C.; Bertrand, P. Conformation Change of Albumin Adsorbed on Polycarbonate Membranes as Revealed by ToF-SIMS. *Langmuir* **2003**, *19*, 6271−6276.
(26) Lhoest, J.-B.; Detrait, E.; Van den Bosch de Aguilar, P.; Bertrand, P. Fibronectin Adsorption, Conformation, and Orientation on Polystyrene Substrates Studied by Radiolabeling, XPS, and ToF SIMS. *J. Biomed. Mater. Res.* **1998**, *41*, 95−103.
(27) Baio, J. E.; Cheng, F.; Ratner, D. M.; Stayton, P. S.; Castner, D. G. Probing Orientation of Immobilized Humanized Anti-Lysozyme Variable Fragment by Time-of-Flight Secondary-Ion Mass Spectrometry. *J. Biomed. Mater. Res., Part A* **2011**, *97A*, 1−7.
(28) Baio, J. E.; Weidner, T.; Baugh, L.; Gamble, L. J.; Stayton, P. S.; Castner, D. G. Probing the Orientation of Electrostatically Immobilized Protein G B1 by Time-of-Flight Secondary Ion Spectrometry, Sum Frequency Generation, and Near-Edge X-ray Adsorption Fine Structure Spectroscopy. *Langmuir* **2012**, *28*, 2107−12.
(29) Henry, M.; Dupont-Gillain, C. C.; Bertrand, P. Characterization of Insulin Adsorption in the Presence of Albumin by Time-of-Flight Secondary Ion Mass Spectrometry and X-ray Photoelectron Spectroscopy. *Langmuir* **2008**, *24*, 458−464.
(30) Henry, M.; Bertrand, P. Surface Composition of Insulin and Albumin Adsorbed on Polymer Substrates as Revealed by Multivariate Analysis of ToF-SIMS Data. *Surf. Interface Anal.* **2009**, *41*, 105−113.
(31) Wang, H.; Castner, D. G.; Ratner, B. D.; Jiang, S. Probing the Orientation of Surface-Immobilized Immunoglobulin G by Time-of-Flight Secondary Ion Mass Spectrometry. *Langmuir* **2004**, *20*, 1877−87.
(32) Norde, W. My Voyage of Discovery to Proteins in Flatland ...and Beyond. *Colloids Surf., B* **2008**, *61*, 1−9.
(33) Walstra, P.; Jenness, R.; Badings, H. T. *Dairy Chemistry and Physics*; John Wiley: New York, 1984; p 467.
(34) Wong, D. W. S.; Camirand, W. M.; Pavlath, A. E. Structures and Functionalities of Milk Proteins. *Crit. Rev. Food Sci. Nutr.* **1996**, *36*, 807−844.
(35) Brownlow, S.; Cabral, J. H. M.; Cooper, R.; Flower, D. R.; Yewdall, S. J.; Polikarpov, I.; North, A. C. T.; Sawyer, L. Bovine b-Lactoglobulin at 1 . 8 Å Resolution — Still an Enigmatic Lipocalin. *Structure* **1997**, *64*, 481−495.
(36) Sauerbrey, G. Use of Quartz Vibrator for Weighing Thin Films on a Microbalance. *Z. Phys.* **1959**, *155*, 206−222.
(37) Wagner, C. D.; Davis, L. E.; Zeller, M. V.; Taylor, J. A.; Raymond, R. H.; Gale, L. H. Empirical Atomic Sensitivity Factors for Quantitative Analysis by Electron Spectroscopy for Chemical Analysis. *Surf. Interface Anal.* **1981**, *3*, 211−225.
(38) Wold, S.; Esbensen, K.; Geladi, P. Principal Component Analysis. *Chemom. Intell. Lab. Syst.* **1987**, *2*, 37−52.
(39) Jackson, J. E. *A User's Guide to Principal Components*; John Wiley & Sons: New York, 1991; Vol. *43*.
(40) Nuzzo, R. G.; Dubois, L. H.; Allara, D. L. Fundamental Studies of Microscopic Wetting on Organic Surfaces. 1. Formation and Structural Characterization of a Self-Consistent Series of Polyfunctional Organic Monolayers. *J. Am. Chem. Soc.* **1990**, *112*, 558−569.
(41) Porter, M. D.; Bright, T. B.; Allara, D. L.; Chidsey, C. E. D. Spontaneously Organized Molecular Assemblies. 4. Structural Characterization of n-Alkyl Thiol Monolayers on Gold by Optical Ellipsometry, Infrared Spectroscopy, and Electrochemistry. *J. Am. Chem. Soc.* **1987**, *109*, 3559−3568.
(42) Genet, M. J.; Dupont-Gillain, C. C.; Rouxhet, P. G. *Medical Applications of Colloids*; Matijevic, E., Ed.; Springer: New York, 2008.
(43) Apte, J. S.; Collier, G.; Latour, R. A.; Gamble, L. J.; Castner, D. G. XPS and ToF-SIMS Investigation of Alpha-Helical and Beta-Strand Peptide Adsorption Onto SAMs. *Langmuir* **2010**, *26*, 3423−32.
(44) Höök, F.; Kasemo, B.; Nylander, T.; Fant, C.; Sott, K.; Elwing, H. Variations in Coupled Water, Viscoelastic Properties, and Film Thickness of a Mefp-1 Protein Film During Adsorption and Cross-Linking: a Quartz Crystal Microbalance With Dissipation Monitoring, Ellipsometry, and Surface Plasmon Resonance Study. *Anal. Chem.* **2001**, *73*, 5796−804.
(45) Höök, F.; Vörös, J.; Rodhal, M.; Kurrat, R.; Böni, P.; Ramsden, J. J.; Textor, M.; Spencer, N. D.; Tengvall, P.; Gold, J.; Kasemo, B. A Comparative Study of Protein Adsorption on Titanium Oxide Surfaces Using In Situ Ellipsometry, Optical Waveguide Lightmode Spectroscopy, and Quartz Crystal Microbalance/Dissipation. *Colloids Surf., B* **2002**, *24*, 155−170.
(46) Briand, E.; Salmain, M.; Compère, C.; Pradier, C.-M. Anti-Rabbit Immunoglobulin G Detection in Complex Medium by PM-RAIRS and QCM Influence of the Antibody Immobilisation Method. *Biosens. Bioelectron.* **2007**, *22*, 2884−90.
(47) Wahlgren, M.; Elofsson, U. Simple Models for Adsorption Kinetics and Their Correlation to the Adsorption of b -Lactoglobulin A and B. *J. Colloid Interface Sci.* **1997**, *188*, 121−129.